Published in final edited form as:
Cancer Cell. 2012 May 15; 21(5): 626–641. doi:10.1016/j.ccr.2012.03.041.

Lunatic Fringe Deficiency Cooperates with the Met/Caveolin Gene Amplicon to Induce Basal-like Breast Cancer

Keli Xu[1,11], **Jerry Usary**[3], **Philaretos C. Kousis**[1], **Aleix Prat**[3], **Dong-Yu Wang**[4], **Jessica R. Adams**[1,6], **Wei Wang**[1], **Amanda J. Loch**[1], **Tao Deng**[5], **Wei Zhao**[3], **Robert Darrell Cardiff**[8], **Keejung Yoon**[9,12], **Nicholas Gaiano**[9], **Vicki Ling**[1,2], **Joseph Beyene**[2,13], **Eldad Zacksenhaus**[5], **Tom Gridley**[10], **Wey L. Leong**[4], **Cynthia J. Guidos**[1,7], **Charles M. Perou**[3], and **Sean E. Egan**[1,6,*]

[1]Program in Developmental and Stem Cell Biology, The Hospital for Sick Children, Toronto, ON, M5G 1L7, Canada

[2]Child Health Evaluative Sciences, The Hospital for Sick Children, Toronto, ON, M5G 1L7, Canada

[3]Lineberger Comprehensive Cancer Center, Departments of Genetics and Pathology, University of North Carolina, Chapel Hill, NC 27599, USA

[4]The Campbell Family Cancer Research Institute and Surgical Oncology Princess Margaret Hospital, and the Department of General Surgery University Health Network, Toronto, ON M5S 1A1, Canada

[5]Division of Cell and Molecular Biology, Toronto General Research Institute, University Health Network, Toronto, ON M5S 1A1, Canada

[6]Department of Molecular Genetics, University of Toronto, Toronto, ON M5S 1A1, Canada

[7]Department of Immunology, University of Toronto, Toronto, ON M5S 1A1, Canada

[8]Center for Comparative Medicine, University of California, Davis, CA 95616, USA

[9]Institute for Cell Engineering, Johns Hopkins University School of Medicine, Baltimore, MD 21205, USA

[10]Center for Molecular Medicine, Maine Medical Center Research Institute, 81 Research Drive, Scarborough, ME 04074, USA

SUMMARY

Basal-like breast cancers (BLBC) express a luminal progenitor gene signature. Notch receptor signaling promotes luminal cell fate specification in the mammary gland, while suppressing stem cell self-renewal. Here we show that deletion of *Lfng*, a sugar transferase that prevents Notch activation by Jagged ligands, enhances stem/progenitor cell proliferation. Mammary-specific

*Correspondence: segan@sickkids.ca DOI 10.1016/j.ccr.2012.03.041.
[11]Present address: Cancer Institute, University of Mississippi Medical Center, 2500 North State Street, Jackson, MS 39216, USA
[12]Present address: College of Biotechnology and Bioengineering, Sungkyunkwan University, Suwon, Gyeonggi-do 440-746, Republic of Korea
[13]Present address: Program in Population Genomics, Department of Clinical Epidemiology and Biostatistics, McMaster University, Hamilton, ON L8S 4L8, Canada

ACCESSION NUMBERS Transcriptional profiling data and aCGH data have been deposited in the GEO database (http://www.ncbi.nlm.nih.gov/geo/; accession numbers GSE28712 and GSE35855, respectively).

SUPPLEMENTAL INFORMATION Supplemental Information includes five figures, one table, and Supplemental Experimental Procedures and can be found with this article online at doi:10.1016/j.ccr.2012.03.041.

deletion of *Lfng* induces basal-like and claudin-low tumors with accumulation of Notch intracellular domain fragments, increased expression of proliferation-associated Notch targets, amplification of the *Met/Caveolin* locus, and elevated Met and Igf-1R signaling. Human BL breast tumors, commonly associated with JAGGED expression, elevated MET signaling, and CAVEOLIN accumulation, express low levels of *LFNG*. Thus, reduced *LFNG* expression facilitates JAG/NOTCH luminal progenitor signaling and cooperates with MET/CAVEOLIN basal-type signaling to promote BLBC.

INTRODUCTION

Patients with BLBC show reduced survival compared to those with more common luminal tumors, and this disease frequently occurs in young patients, as well as in women with African ancestry. Basal-like tumors express markers of myoepithelium, but show a gene expression signature related to that of luminal progenitor cells (Cheang et al., 2008; Lim et al., 2009; Perou and Børresen-Dale, 2011; Prat et al., 2010). Indeed, luminal progenitors may be the cell-of-origin for most BLBC (Molyneux et al., 2010). In the mouse system, activated Notch1 can induce commitment of mammary stem cells (MaSC) into luminal progenitors, and promote proliferation of luminal progenitor cells in vitro and in vivo (Bouras et al., 2008). Similarly in humans, increased *NOTCH3* expression and function can promote luminal progenitor cell fate specification, at least in vitro (Raouf et al., 2008).

On the basis of studies with the Mouse Mammary Tumor Virus (MMTV), which can induce mammary tumor formation through insertional activation of Notch genes, a role for Notch signaling in human breast cancer was anticipated (Callahan and Smith, 2000). Most human breast tumors express Notch ligands and receptors (Parr et al., 2004; Pece et al., 2004; Reedijk et al., 2005; Stylianou et al., 2006). High-level expression of the *JAGGED1* ligand, as well as *NOTCH1* and/or *NOTCH3*, is associated with poor overall survival (Reedijk et al., 2005). Recent studies reveal that signaling through multiple Notch receptors activates proliferation and/or survival of breast cancer cells (Harrison et al., 2010; Haughian et al., 2012; Osipo et al., 2008; Sansone et al., 2007; Yamaguchi et al., 2008). Interestingly, JAGGED-dependent Notch pathway activation has been associated with triple negative ($ER\alpha^-$, PR^- and $HER2^-$) tumors, and specifically with basal-like tumors and cell lines (Cohen et al., 2010; Dong et al., 2010; Haughian et al., 2012; Lee et al., 2008a, 2008b; Leong et al., 2007; Reedijk et al., 2008; Sansone et al., 2007).

Met, a cell surface tyrosine kinase receptor involved in epithelial-mesenchymal transition, is frequently expressed at high levels in BLBC (Elsheikh et al., 2008; Gastaldi et al., 2010; Lu et al., 2008; Ponzo and Park, 2010; Ravid et al., 2005; Salani et al., 2008; Savage et al., 2007), and many basal-like tumors show elevated Met signaling (Hochgräfe et al., 2010). In addition, Caveolin1 and 2, which facilitate Igf-1R signaling, are also overexpressed (Elsheikh et al., 2008; Gastaldi et al., 2010; Lu et al., 2008; Ponzo and Park, 2010; Ravid et al., 2005; Salani et al., 2008; Savage et al., 2007). Interestingly, the genes coding for MET, CAV1, and CAV2 are located in the same region of Chromosome 7q31 and this locus is overexpressed in many BLBC (Elsheikh et al., 2008; Gastaldi et al., 2010; Ponzo and Park, 2010; Savage et al., 2007).

Fringe proteins are N-acetylglucosamine transferases that modify Notch receptors to control ligand-mediated activation (Haines and Irvine, 2003). These proteins enhance Notch activation by Delta-family ligands, while inhibiting Notch activation by Serrate/Jagged ligands (Haines and Irvine, 2003). *Lfng*, one of three Fringe genes in mammals, controls Notch signaling in many developing tissues (Cohen et al., 1997; Johnston et al., 1997). Interestingly, *LFNG* is expressed at high levels in MaSC and/or bipotent progenitor cells of

the human breast (Raouf et al., 2008). However, its role in the regulation of Notch signaling of the developing or adult mammary gland remains unknown, as is its potential for restricting Notch-dependent oncogenic signaling in this context. In this study, we used conditional mutant mice to define the function of *Lfng* in mammary epithelium. In addition, we tested for its expression and potential role in human breast cancer.

RESULTS

A Lfng Expression Boundary in Mammary Development

To define where and when Notch is activated in the developing mammary gland, we used LacZ knock-in mice for various Notch pathway genes. Typically, boundaries between Fringe-expressing cells and nonexpressing cells are sites of consequential Notch signaling (Irvine, 1999). Therefore, we examined *Lfng* expression by performing X-gal staining on mammary glands from six-week-old $Lfng^{LacZ/+}$ virgin females (Zhang and Gridley, 1998). Interestingly, *Lfng* expression was restricted to basal cells, in particular to cap cells of terminal end buds (TEBs) (Figure 1A), which have MaSC activity (Bai and Rohrschneider, 2010). This result is consistent with studies on cells purified from the human mammary gland, which show that *LFNG* expression is > 20-fold enriched in stem and/or bipotent progenitor cells as compared with luminal restricted progenitors (Raouf et al., 2008). Two Notch ligands, *Dll1* and *Jagged1*, show distinct expression at this stage. Weak X-gal staining from a $Dll1^{lacZ/+}$ allele (Hrabě de Angelis et al., 1997) was observed in cap cells of the mammary TEB. In contrast, their basally located myoepithelial descendants showed intense staining. X-gal staining in pubescent $Jagged1^{\beta-Geo/+}$ (Xu et al., 2010) mice was strongest in stromal cells surrounding each TEB (Figure 1A).

In mature adults, after TEB regression, $Lfng^{lacZ}$ expression was barely detected, while $Dll1^{lacZ}$ expression remained strong in myoepithelial cells. Interestingly, *Jagged1* expression switched from stroma to myoepithelium in the mature gland (Figure 1A). *JAGGED1* expression is also high in basal cells of the mature human gland (Reedijk et al., 2005). Next, we used antibodies to stain for Notch1 and Notch4, which were expressed at low levels in luminal and basal cells, respectively (Figure S1A available online). Using *β-Geo/+* knock-in mice (Xu et al., 2010), *Notch3* expression was found to be high in body cells of the TEB, as well as in luminal epithelial cells of mature ducts, whereas *Notch2* expression was strong in stroma and weak in epithelium (Figure S1B). These data are consistent with recent Notch ligand and receptor expression analysis by rtPCR and immunohistochemistry (Bouras et al., 2008; Raafat et al., 2011; Raouf et al., 2008).

Lfng Controls Notch Activation and Suppresses Mammary Epithelial Proliferation

Fringe controls Notch activation at compartment boundaries in the developing fruit fly (Irvine, 1999). Our expression analysis in the mammary gland reveals a similar boundary at the TEB-ductal junction, where *Lfng* may differentially regulate Notch activation induced by Dll1 and/or Jagged1. To define Lfng function in this context, we analyzed mammary development in *Lfng* mutant mice. Whole-mount analysis showed evidence of epithelial hyperplasia in virgin mammary glands from *Lfng* mutants (Figure 1B). Sections from mutant and control glands were stained with antibodies against luminal and basally restricted cytokeratins, keratin 8 (K8) and 14 (K14), respectively. Most mutant glands showed decreased K8 expression in body cells of the TEB. Also, multiple layers of $K14^+$ basal cells were observed in some locations. Cells did not co-express K8 and K14 in wild-type or mutant glands during puberty (Figure 1C). We next tested for altered cell proliferation by staining for Ki67. Indeed, *Lfng* mutant glands showed increased cell proliferation in mature ducts (Figure 1D).

Fringe proteins control Notch signaling by enhancing Delta-while inhibiting Serrate/Jagged-mediated activation (Haines and Irvine, 2003). Based on high-level *Lfng* expression in cap cells of the TEB, and the known cell autonomous function of Fringe proteins (Panin et al., 1997), Lfng likely facilitates Dll-mediated Notch signaling or blocks Jagged1-mediated Notch activation in MaSC and/or bipotential progenitors of the cap layer. The Transgenic Notch Reporter (TNR) mouse has an artificial Notch-responsive promoter with multiple RBPJκ-binding sites regulating expression of eGFP (Duncan et al., 2005). This mouse has been used successfully to study Notch/p63 interaction in the developing mammary gland (Yalcin-Ozuysal et al., 2010). Therefore, to test for alterations in Notch signaling associated with *Lfng* deletion, we crossed TNR reporter mice with *Lfng* mutants. To follow Notch signaling at multiple levels within the developmental hierarchy, lineage-depleted mammary epithelial cells were stained for surface markers CD24, CD49f, CD61, and Sca1. Remarkably, *Lfng* null glands showed a more than 2-fold (2.37 ± 0.07, $p < 0.05$) enrichment of $CD24^{+}CD49f^{hi}$ cells, a population known to contain mammary stem/early progenitor cells (Figure 1E). We gated on this population and found that most cells were $CD61^{+}Sca1^{-}$, characteristic of MaSC (Visvader, 2009) (Figure 1E). In some cases this was associated with decreased numbers of $CD24^{hi}C49f^{+}$ $CD61^{+}$ luminal progenitor cells (Figure 1E). Thus, our flow cytometry analysis indicated that deletion of *Lfng* caused accumulation of stem/bipotent progenitor cells, likely at the expense of luminal progenitor cells in the developing mammary gland. Interestingly, $Lfng^{-/-}$; *TNR* mutants showed 40% decrease in GFP^{+} lineage-depleted mammary epithelial cells as compared to $Lfng^{+/+ \text{ or } +/-}$; *TNR* controls (Figure S1C). Specifically, in mutant mice, fewer cells with active Notch signaling were observed in MaSC/early progenitor-containing ($CD24^{+}CD49f^{hi}$) and luminal progenitor-containing ($CD24^{hi}$ $CD49f^{+}$) compartments (Figure S1D) (Shackleton et al., 2006; Stingl et al., 2006). Thus, deletion of *Lfng* leads to decreased Notch signaling in MaSC and progenitors in puberty (likely as a result of reduced Dll1-mediated Notch activation at this stage), and is associated with expansion of the immature cell compartment. These data are consistent with those of Bouras et al., who showed that shRNA-mediated knockdown of *RBPJκ*, and thus disruption of canonical Notch signaling, caused expansion of the $CD24^{+}CD29^{hi}$ compartment (note: this is the same as the $CD24^{+}CD49f^{hi}$ compartment), and promotion of MaSC self-renewal (Bouras et al., 2008).

Lfng Is a Suppressor of Basal-like Tumor Formation in the Mouse Mammary Gland

Next, we tested for *Lfng* function by generating a Cre-conditional *Lfng* mutant mouse (Xu et al., 2010). This mouse was crossed to MMTV-Cre line A, which shows robust expression in mammary epithelium (Wagner et al., 1997). Many $Lfng^{flox/flox}$; *MMTV-Cre* mutant mice developed mammary tumors starting at 10 months of age (Figure 2A). Histological analysis revealed three types of *Lfng* mutant tumors: approximately 60% showed glandular differentiation (type I); one-third mainly consisted of mesenchymal/spindle-shaped cells (type II); and about 5% had areas containing multinucleated giant cells (type III) (Figure 2B). All three histological types were triple-negative (ERα-, PR-, Her2/Neu-negative) (Figure 2C and data not shown), and highly proliferative (Figure 2D). Interestingly, tumors of all three types had cells co-expressing luminal (K8) and basal markers (K14). Notably, type I tumors contained a higher percentage (75.3% versus 16.8% in type II) of cells expressing one or both lineage-specific keratin (Figure 2E).

Next, we used transcriptional profiling to define molecular subtype for 11 *Lfng* mutant tumors (Herschkowitz et al., 2007). Interestingly, in unsupervised cluster analysis, these tumors grouped with basal-like and claudin-low models but were otherwise quite unique. Specifically, six type I tumors clustered together with *Brca1/p53* tumors, DMBA-induced tumors and Wap-$SV40T^{121}$-induced tumors, all of which are related to BLBC, whereas five spindle/EMT or type II *Lfng* mutant mammary tumors clustered nearby, together with

DMBA-induced spindle tumors as well as with *Brca1/p53* tumors, which have previously been identified as claudin-low (Herschkowitz et al., 2007) (Figures 3A and 3B). The claudin-low signature is related to that observed in MaSCs (Hennessy et al., 2009). Interestingly, many mouse mammary tumors that were induced by activated Met cluster with similar basal-like mouse models (Ponzo et al., 2009). We also performed enrichment map analysis to identify differentially expressed gene sets in *Lfng*$^{flox/flox}$*; MMTV-Cre* mammary tumors as compared to those expressed in other mouse breast cancer models. Interestingly, gene sets implicated in leukocyte activation and proliferation, inflammation, cytokine and chemokine signaling, as well as extracellular matrix remodeling were overrepresented in *Lfng* mutant tumors (Figure 3C and Table S1).

We next analyzed tumors by flow cytometry. *Lfng* mutant tumors were composed of cells with marker profiles that were distinct from profiles seen in the normal mammary gland. As discussed previously, the characteristic mammary epithelial profile includes CD24^{+}CD49f^{hi} cells enriched for MaSC/bipotent progenitors, CD24^{hi}CD49f^{+} cells that are enriched for luminal progenitors, with a third compartment of CD24^{-}CD49f^{-} cells. In contrast, type I *Lfng* mutant tumors had an increased fraction of CD49f^{+} cells, approximately half of which expressed CD24 (Figure 4A). Most of the CD49f^{+} cells also expressed CD61, with lower expression of Sca1 noted. Finally, there was an increased number of CD24^{+}CD61^{+} cells and most of these were CD49f^{+}Sca1^{-}, suggesting that a luminal progenitor-like compartment is expanded in these tumors (Figures 4B and S2A) (Visvader, 2009; Visvader and Smith, 2011). Next, fluorescence-activated cell sorting was used to fractionate tumor cells and to test for tumor initiating activity. Specifically, we separated type I tumors into three distinct populations (CD24^{+}CD49f^{+}, CD24^{-}CD49f^{-}, and CD24^{-}CD49f^{+}) and injected matrigel suspensions of each into mammary fat pads of FVB recipient mice. Most tumor initiating activity was found within the CD24^{+} CD49f^{+} luminal progenitor-like population (Figure 4C).

Immunohistochemical analysis showed type I tumors also expressed high levels of CD61, contained Aldh1^{+} cells, and expressed low levels of Gata3 (Figures 4D and S2B) (Ginestier et al., 2007; Visvader, 2009; Visvader and Smith, 2011). Type II tumors show fewer CD61^{+} cells, and were almost completely negative for Aldh1. However, Vimentin and Twist, two markers associated with EMT, were broadly expressed in type II, but not type I, tumors (Figure 4D). Phospho-Akt, a marker of PI3K signaling, was evident in type II tumors and at a somewhat lower level in type I tumors (Figure 4D). Thus, based on histology, transcriptional profiling, flow cytometry and marker analysis, type I lesions were basal-like tumors with features of luminal progenitors (Cheang et al., 2008; Perou and Børresen-Dale, 2011), and type II were similar to claudin-low tumors with EMT-like features, a phenotype associated with MaSC-like cells (Cardiff, 2010; Taube et al., 2010).

Because Lfng regulates Notch signaling in mammary epithelium as shown previously, we tested for altered expression of known Notch target genes in these tumors. Indeed, all 11 *Lfng*$^{flox/flox}$*; MMTV-Cre* mammary tumors showed reduced expression of *Hey1*, *Hey2*, and *Notch3*, but elevated expression of *Dll4* and the Notch target genes *uPA*, *c-Myc*, and *Cyclin D1* (Cohen et al., 2010; Klinakis et al., 2006; Shimizu et al., 2011) (Figure 5A). As for other models, high-level expression of *Hey1*, *Hey2*, *Notch3*, *c-Myc*, *Cyclin D1*, and *Notch4* (*Int3*), as well as low-level expression of *p63* and *Dll1* was observed in tumors induced by activated Notch4 (Wap-*Int-3*). In contrast, low-level expression of *Hey1*, *Notch1*, *c-Myc* (endogenous), *Cyclin D1*, *p63*, and *Dll1* was observed in MMTV-Myc tumors. Finally, *Hey1* was highly expressed in Her2/Neu and Polyoma Middle T-induced tumors (Figure 5A).

To directly test for activation of Notch signaling in *Lfng*$^{flox/flox}$;*MMTV-Cre* mammary tumors, we performed western blot analysis using antibodies that recognize N-terminal sequences of cleavage-generated intracellular domain (ICD) fragments from Notch1 and 2. Indeed, higher levels of Notch1^{ICD} and Notch2^{ICD} were present in *Lfng* mutant tumors as compared to control non–tumor-bearing glands from the same animal (Figure 5B). Specific antibodies to detect murine Notch3^{ICD} and Notch4^{ICD} are currently unavailable; however, expression and processing of both proteins were changed in *Lfng* mutant tumors (Figure S3). For Notch4, increased accumulation of a C-terminal fragment consistent with Notch4^{ICD} was observed (Figure S3). Finally, Jagged1 protein was expressed in *Lfng* mutant tumors, as were the protein products of Notch target genes, *Cyclin D1* and *c-Myc* (Figure 5C). Thus, *Lfng* gene deletion results in Notch activation in these tumors, and is consistent with induction of Jagged/Notch target genes, *CyclinD*1 and *c-Myc*.

Met/Caveolin Gene Amplification and Signaling in *Lfng* Mutant Tumors

Next, to identify cooperative events in *Lfng* mutant tumors, we performed aCGH (array comparative genomic hybridization) on DNA isolated from 5 *Lfng* conditional mutant tumors as compared to non-tumor DNA isolated from control tissue. While copy number gains and losses were noted in many regions across the genome, the only common abnormality involved amplification of a small locus at chromosome 6A2 (Figures S4A and S4B). This was observed in 4 out of 5 tumor samples, the exception being a *Lfng*$^{flox/+}$;*MMTV-Cre* mammary tumor. The overlapping region with copy number gains in each of the four tumors contained 13 genes including the tyrosine kinase *Met*, and neighboring *Cav1* and *2* genes (Figure 6A). This locus is amplified and/or overexpressed in BLBC in humans and in mammary tumors from *Brca1*$^{\delta 11/co}$; *p53*$^{+/-}$; *MMTV-Cre* mice (Savage et al., 2007; Smolen et al., 2006). To determine which, if any, of these genes were overexpressed in *Lfng* mutant tumors, we screened our transcriptional profiling data for expression of genes within this region. Indeed, expression of several, including *Met*, *Cav1* and *2*, was significantly elevated in *Lfng* mutant tumors (Figure 6B). Interestingly, high-level *MET* expression has been noted in aggressive human breast cancer, particularly in breast tumors with EMT features (Gastaldi et al., 2010; Ponzo and Park, 2010), and expression of oncogenic *Met* can induce basal-like mammary tumors in transgenic mice (Graveel et al., 2009; Ponzo et al., 2009). We next used western analysis to test for elevated Met accumulation and activation in *Lfng* mutant tumors. As shown in Figure 6C, *Lfng* mutant tumors showed dramatically increased Met expression and activation. Overexpressed Met could still depend on HGF ligand for activation. Indeed, *Hgfa*, was identified as overrepresented in gene expression signatures from *Lfng* mutant tumors in comparison to other mouse models of breast cancer analyzed (Table S1), and HGFα expression was detected by western analysis of *Lfng* mutant tumors (data not shown). Next, we analyzed Caveolin 1/2 expression in *Lfng* tumors. In the normal mammary gland, Caveolin 1 is very highly expressed in endothelial cells, adipocytes, and basally localized myoepithelium. High-level expression was also seen in type I and II tumor cells (Figure 6D). We analyzed Caveolin 2 expression by western blot, and in each case, it was elevated in tumor cells in comparison to nontumorous mammary tissue from the same animal (Figure 6E). Caveolin expression has been linked to enhanced Insulin and Igf-1R signaling (Lu et al., 2008; Ravid et al., 2005; Salani et al., 2008), and elevated Igf-1R signaling can induce mammary tumors in mice (Jones et al., 2007). We therefore analyzed InsR and Igf-1R signaling at the level of Irs1/2 tyrosine phosphorylation. Indeed, Irs tyrosine phosphorylation was elevated in *Lfng* mutant mammary tumors (Figure 6E). Thus, *Lfng* mutant tumors have selected for activation of receptors that are more highly expressed or active in basal cells (Hvid et al., 2011; Niranjan et al., 1995).

Low-Level *LFNG* Expression Is a Hallmark of Basal-like Breast Cancer in Humans

Because deletion of *Lfng* caused basal-like and claudin-low mammary tumors in mice, we analyzed *LFNG* expression in human breast cancer. First, we screened publically available gene expression data from 676 human breast cancers with linked clinical-pathological information. Interestingly, reduced *LFNG* expression was associated with high tumor grade, with ERα/PR/HER2 triple-negative status, and most significantly, with the basal-like molecular subtype (Figures S5A and S5B). To the contrary, elevated *LFNG* expression was noted in ER^+ tumors and $HER2^+$ tumors (Figures S5A and S5B). Nevins and colleagues have recently identified gene expression signatures for activation of signaling pathways in breast cancer (Gatza et al., 2010). We therefore tested for activation of these pathways in relation to *LFNG* gene expression. Several oncogenic pathways including those associated with a high rate of proliferation (Myc and E2F1), as well as stem cell signaling (β-catenin), show increased activity in tumors with low *LFNG* expression, whereas the p53 pathway activity is significantly depressed in $LFNG^{low}$ tumors (Figure S5B). As *Met* was amplified and overexpressed in our *Lfng* mutant mammary tumors, we also tested for *MET* expression. As previously noted, basal-like and triple negative breast tumors expressed elevated levels of MET (Figure S5B and S5C) (Graveel et al., 2009; Ponzo et al., 2009). Perhaps not surprisingly, low *LFNG* expression was correlated with elevated *MET* levels (Figure S5C).

Finally, a number of studies have highlighted a potential role for Notch receptor signaling in human breast cancer. Therefore, we performed cluster analysis on the UNC publicly available microarray data set (UNC337, GSE18229), and evaluated expression of NOTCH pathway genes in each subtype (Prat et al., 2010). Once again, low-level *LFNG* expression was noted in basal-like tumors from this cohort, and also in a group of claudin-low tumors (Figures 7A and 7B). *HES1*, and to a lesser extent *HEY1*, showed reduced expression in a subset of basal tumors (Figure 7A). In contrast, *c-Myc* and *NOTCH1* expression were elevated in BLBC (Figures 7A and 7B). Thus, *LFNG* expression is consistently low in human basal-like and a subset of claudin-low breast cancers. These data help explain how Jagged-mediated Notch activation stimulates proliferation (Cohen et al., 2010) as well as invasion (Shimizu et al., 2011) of BLBC and other triple-negative breast tumors.

DISCUSSION

With the discovery of Notch4 as a target in MMTV-induced mammary tumor formation, it became clear that elevated Notch signaling was oncogenic in mammary epithelium (Callahan and Smith, 2000). Indeed, translocations that activate *NOTCH1* or *2* have been identified in some triple-negative breast cancers and cell lines (Robinson et al., 2011). In this study we have identified a role for *Lfng* deletion (mouse) or downregulation (human) in BLBC, associated with activation of $Notch^{ICD}$ accumulation and induction of oncogenic Notch target gene expression. Multiple Notch receptors are expressed in the mammary gland and several of these are believed to function in breast cancer (Harrison et al., 2010; Haughian et al., 2012; Osipo et al., 2008; Sansone et al., 2007; Yamaguchi et al., 2008). Based on accumulation of luminal progenitor-like cells in *Lfng* mutant basal-like tumors, our data reinforce the finding that elevated Notch signaling enhances proliferation of this compartment (Bouras et al., 2008). Interestingly, a low level of *LFNG* is observed in the vast majority of BLBCs (Figure 7). It will be important to see how these tumors compare in phenotype to the small fraction of triple-negative tumors with Notch-activating translocations (Robinson et al., 2011).

Deletion of *Lfng* in our conditional mutant mice results in reduced expression of the Notch reporter gene during puberty. Based on the known function of Fringe proteins to enhance Delta ligand–mediated signaling, these data suggest that Dll1, expressed in myoepithelial

cells, functions to activate Notch in *Lfng*-expressing MaSCs or bipotent progenitors. In adults, *Jagged1* expression is enhanced within the epithelial compartment (Figure 1) (Reedijk et al., 2005). Loss of *Lfng* in this setting would be expected to increase Jagged/Notch signaling and to induce luminal cell fate commitment as well as proliferation of luminal progenitors (Bouras et al., 2008). It is this effect, in older animals, that is likely responsible for establishing both lineage bias and progenitor compartment expansion to set the stage for transformation.

Human BLBCs contain dozens of mutations that presumably cooperate to transform mammary progenitor cells (Ding et al., 2010). Recent data indicate that cooperative interactions occur between mutations in a number of tumor suppressors, including *RB1*, *TP53*, *BRCA1*, *PTEN*, and *PTPN12* (Carey et al., 2010; Foulkes et al., 2010; Herschkowitz et al., 2008; Holstege et al., 2010; Jiang et al., 2010, 2011; Kobayashi, 2008; Rakha et al., 2008; Saal et al., 2008; Sun et al., 2011). Despite this, it has not been clear how oncogenic pathways interact to control lineage in basal tumors. As a first step to define cooperative pathways in *Lfng* mutant tumors, we performed aCGH analysis and found *Met/Cav* gene amplification and enhanced signaling to represent a common event in this context. Indeed, low-level *LFNG* expression and elevated MET signaling are both associated with BLBC in humans (Gastaldi et al., 2010; Ponzo and Park, 2010). Interestingly, this same amplicon is selected for in brain tumors that occur in *Pten/p53* conditional mutant mice, but not in brain tumors from mice with conditional deletion of *Pten*, *p53*, and *Rb* (Chow et al., 2011), suggesting that *Met/Cav* gene amplification/overexpression may perform similar oncogenic functions as *Rb* gene deletion, an event also associated with BLBC in humans and mice (Herschkowitz et al., 2008; Jiang et al., 2010). The consistent selection for amplification of the *Met/Cav* locus in *Lfng* mutant tumors is striking, and speaks to an emerging concept in cancer whereby genes that function synergistically to enhance signaling through a specific oncogenic signaling pathway will frequently be co-selected during tumor formation or progression. For example, the chromosome 17q amplicon in $HER2^+$ breast tumors encodes the HER2 receptor and also the Grb7 adaptor protein, which binds to HER2 protein to facilitate signal transduction (Andrechek et al., 2003; Stein et al., 1994). In addition, the 9p24 amplicon associated with mediastinal B cell lymphoma contains several genes that interact synergistically to enhance IL-13 signaling (Rui et al., 2010). The consistent selection for amplification of the *Met/Cav* gene locus in *Lfng* mutant tumors, and common overexpression of this locus in human BLBC, also leads to synergistic interactions. As depicted in Figure 8, *Lfng* gene loss or reduced expression of *LFNG* in human tumors cooperates with *Met* and *Cav1/2* gene amplification at multiple levels. First, elevated Notch signaling as a result of decreased *Lfng* function, promotes specification and proliferation of luminal progenitors (Bouras et al., 2008). In addition, *Met* amplification would naturally result in elevated Met signaling. This effect should be enhanced through absence of Hes/Hey-mediated silencing of the *Met* gene promoter (Stella et al., 2005). Finally, Caveolin1/2 overexpression would be expected to enhance signaling through the insulin receptor and/or Igf-1R (Lu et al., 2008; Ravid et al.,2005; Salani et al., 2008). Indeed, our *Lfng* mutant model of BLBC shows elevated Notch signaling to proliferation/invasion Notch target genes as well as reduced Hes/Hey expression, together with elevated Met and InsR/Igf-1R signaling. Interestingly, elevated Notch signaling and *Met/Cav* overexpression could potentially also connect through induction of uPA (Lee et al., 2006; Monaghan-Benson et al., 2008; Shimizu et al., 2011) and activation of HGF (Naldini et al., 1995). The specific combination of oncogenic mutations would therefore have the effect of promoting a luminal progenitor fate with lower integrin expression, and therefore reduced survival signaling from the basement membrane. The selection for elevated Met and InsR/Igf-1R signaling can thus provide a basal survival-type signal for these luminal progenitor tumor cells. Thus, combination therapy targeting Notch, Met and InsR/Igf-1R or other elements in this hybrid

luminal/basal signaling network may prove effective for treatment of BLBC with low *LFNG* gene expression plus overexpression of the *MET/CAV* locus on chromosome 7q31.

EXPERIMENTAL PROCEDURES

Mice

Mice were housed under standard condition and protocols approved by animal care committees at the Hospital for Sick Children and Toronto Center for Phenogenomics. The specific mice used for this study are described elsewhere (Duncan et al., 2005; Hrabě de Angelis et al., 1997; Xu et al., 2010; Zhang and Gridley, 1998). Note, the $Lfng^{-}$ null allele was generated through expression of Cre in the germline of female $Lfng^{flox/+}$; *MMTV-Cre* mice. $Lfng^{flox/flox}$; MMTV-Cre experimental animals were generated by crossing $Lfng^{flox/flox}$ females with $Lfng^{flox/flox}$; MMTV-Cre males, which did not result in Cre-mediated deletion in the germline.

Mammary Gland Whole-Mounts, X-Gal Staining, Immunohistochemistry, and Western Analysis

These techniques were performed as per standard protocols and are described in Supplemental Experimental Procedures.

Flow Cytometry and Tumor Cell Transplantation

Mouse mammary tissues were dissociated in Epicult-B medium plus collagenase/hyaluronidase (StemCell Technologies), and single cell suspensions were generated according to manufacturer's protocols. Lineage-depleted (Lin^{-}) mammary epithelial cells were prepared using a Mouse Mammary Stem Cell Enrichment Kit (StemCell Technologies). Lin^{-} single cells were suspended in HBSS with calf serum and HEPES, and stained with saturating concentrations of fluorochrome-conjugated antibodies as listed in Supplemental Experimental Procedures. Fluorescence was recorded using BD LSR-II flow cytometer and analyzed with FlowJo 9.1 (Treestar). Dead cells were excluded based on propidium iodide staining. Distinct populations of tumor cells were serially diluted, suspended in matrigel, and then injected into the mammary fat pad of 4-week-old FVB mice (Liu et al., 2007).

Array Comparative Genomic Hybridization

Genomic DNAs were purified using DNAeasy kits (QIAGEN) combined with phenol-chloroform extraction. Array CGH was conducted at the Center for Applied Genomics, Hospital for Sick Children. Briefly, 2.0 mg genomic DNA was labeled using a BioPrime kit (Invitrogen), hybridized to Agilent mouse 1 × 1M CGH arrays, and scanned. Genomic DNA from non-tumor mammary tissue of the same animal was used as reference for tumor samples.

Microarray Gene Expression Analysis

Mouse mammary tumor RNA was purified using an RNeasy mini Kit (QIAGEN). Microarray hybridizations were performed as described in Herschkowitz et al. except that samples were hybridized to custom 180K Agilent microarrays (BARCODE25503) and were scanned using an Agilent Microarray Scanner with Feature Extraction software (Herschkowitz et al., 2007). Analysis of the North Carolina breast cancer data set has been described (Prat et al., 2010). See Supplemental Experimental Procedures for gene expression analysis of mouse mammary tumors and analysis of LFNG expression in 676 human breast cancers.

Statistics

All data are presented as mean ± standard error (SE). For two group comparisons, two-tailed Student's t test was used. For fold changes compared to 1, one-tailed one sample t test was used. A p value of 0.05 or less was considered statistically significant. Mouse tumor-free survival was analyzed by the Kaplan-Meier method and compared by a nonparametric log-rank test. Frequency of tumor-initiating cells was calculated using L-Calc software (StemCell Technologies).

Supplementary Material

Refer to Web version on PubMed Central for supplementary material.

Acknowledgments

The authors thank Chao Lu, Jo-Anne Herbrick, Steve Scherer, and Jeff MacDonald in the Center for Applied Genomics at the Hospital for Sick Children as well as technicians at The Toronto Center for Phenogenomics. We also thank members of the Egan and Zacksenhaus labs and colleagues at the Hospital for Sick Children. Finally, we thank Dr. Daniele Merico for bioinformatic analysis, Dr. Jeff Liu for TIC calculations, Drs. Morag Park and Sam Aparicio for discussions on BLBC, and anonymous reviewers for helpful comments on the manuscript. K.X. was supported by a CIHR fellowship. S.E.E.'s lab has been supported by funds from the Canadian Cancer Society Research Institute, from Susan G. Komen for the Cure, and from Genome Canada. Work in C.M.P.'s lab has been supported by funds from the NCI Breast SPORE program (P50-CA58223-09A1), by R01-CA138255 and R01-CA148761, by the Sociedad Española de Oncología Médica (SEOM), and by the Breast Cancer Research Foundation.

REFERENCES

Andrechek ER, Laing MA, Girgis-Gabardo AA, Siegel PM, Cardiff RD, Muller WJ. Gene expression profiling of neu-induced mammary tumors from transgenic mice reveals genetic and morphological similarities to ErbB2-expressing human breast cancers. Cancer Res. 2003; 63:4920–4926. [PubMed: 12941816]

Bai L, Rohrschneider LR. s-SHIP promoter expression marks activated stem cells in developing mouse mammary tissue. Genes Dev. 2010; 24:1882–1892. [PubMed: 20810647]

Bouras T, Pal B, Vaillant F, Harburg G, Asselin-Labat ML, Oakes SR, Lindeman GJ, Visvader JE. Notch signaling regulates mammary stem cell function and luminal cell-fate commitment. Cell Stem Cell. 2008; 3:429–441. [PubMed: 18940734]

Callahan R, Smith GH. MMTV-induced mammary tumorigenesis: gene discovery, progression to malignancy and cellular pathways. Oncogene. 2000; 19:992–1001. [PubMed: 10713682]

Cardiff RD. The pathology of EMT in mouse mammary tumorigenesis. J. Mammary Gland Biol. Neoplasia. 2010; 15:225–233. [PubMed: 20521088]

Carey L, Winer E, Viale G, Cameron D, Gianni L. Triple-negative breast cancer: disease entity or title of convenience? Nat. Rev. Clin. Oncol. 2010; 7:683–692. [PubMed: 20877296]

Cheang MC, Voduc D, Bajdik C, Leung S, McKinney S, Chia SK, Perou CM, Nielsen TO. Basal-like breast cancer defined by five biomarkers has superior prognostic value than triple-negative phenotype. Clin. Cancer Res. 2008; 14:1368–1376. [PubMed: 18316557]

Chow LM, Endersby R, Zhu X, Rankin S, Qu C, Zhang J, Broniscer A, Ellison DW, Baker SJ. Cooperativity within and among Pten, p53, and Rb pathways induces high-grade astrocytoma in adult brain. Cancer Cell. 2011; 19:305–316. [PubMed: 21397855]

Cohen B, Bashirullah A, Dagnino L, Campbell C, Fisher WW, Leow CC, Whiting E, Ryan D, Zinyk D, Boulianne G, et al. Fringe boundaries coincide with Notch-dependent patterning centres in mammals and alter Notch-dependent development in Drosophila. Nat. Genet. 1997; 16:283–288. [PubMed: 9207795]

Cohen B, Shimizu M, Izrailit J, Ng NF, Buchman Y, Pan JG, Dering J, Reedijk M. Cyclin D1 is a direct target of JAG1-mediated Notch signaling in breast cancer. Breast Cancer Res. Treat. 2010; 123:113–124. [PubMed: 19915977]

Ding L, Ellis MJ, Li S, Larson DE, Chen K, Wallis JW, Harris CC, McLellan MD, Fulton RS, Fulton LL, et al. Genome remodelling in a basal-like breast cancer metastasis and xenograft. Nature. 2010; 464:999–1005. [PubMed: 20393555]

Dong Y, Li A, Wang J, Weber JD, Michel LS. Synthetic lethality through combined Notch-epidermal growth factor receptor pathway inhibition in basal-like breast cancer. Cancer Res. 2010; 70:5465–5474. [PubMed: 20570903]

Duncan AW, Rattis FM, DiMascio LN, Congdon KL, Pazianos G, Zhao C, Yoon K, Cook JM, Willert K, Gaiano N, Reya T. Integration of Notch and Wnt signaling in hematopoietic stem cell maintenance. Nat. Immunol. 2005; 6:314–322. [PubMed: 15665828]

Elsheikh SE, Green AR, Rakha EA, Samaka RM, Ammar AA, Powe D, Reis-Filho JS, Ellis IO. Caveolin 1 and Caveolin 2 are associated with breast cancer basal-like and triple-negative immunophenotype. Br. J. Cancer. 2008; 99:327–334. [PubMed: 18612310]

Foulkes WD, Smith IE, Reis-Filho JS. Triple-negative breast cancer. N. Engl. J. Med. 2010; 363:1938–1948. [PubMed: 21067385]

Gastaldi S, Comoglio PM, Trusolino L. The Met oncogene and basal-like breast cancer: another culprit to watch out for? Breast Cancer Res. 2010; 12:208. [PubMed: 20804567]

Gatza ML, Lucas JE, Barry WT, Kim JW, Wang Q, Crawford MD, Datto MB, Kelley M, Mathey-Prevot B, Potti A, Nevins JR. A pathway-based classification of human breast cancer. Proc. Natl. Acad. Sci. USA. 2010; 107:6994–6999. [PubMed: 20335537]

Ginestier C, Hur MH, Charafe-Jauffret E, Monville F, Dutcher J, Brown M, Jacquemier J, Viens P, Kleer CG, Liu S, et al. ALDH1 is a marker of normal and malignant human mammary stem cells and a predictor of poor clinical outcome. Cell Stem Cell. 2007; 1:555–567. [PubMed: 18371393]

Graveel CR, DeGroot JD, Su Y, Koeman J, Dykema K, Leung S, Snider J, Davies SR, Swiatek PJ, Cottingham S, et al. Met induces diverse mammary carcinomas in mice and is associated with human basal breast cancer. Proc. Natl. Acad. Sci. USA. 2009; 106:12909–12914. [PubMed: 19567831]

Haines N, Irvine KD. Glycosylation regulates Notch signalling. Nat. Rev. Mol. Cell Biol. 2003; 4:786–797. [PubMed: 14570055]

Harrison H, Farnie G, Howell SJ, Rock RE, Stylianou S, Brennan KR, Bundred NJ, Clarke RB. Regulation of breast cancer stem cell activity by signaling through the Notch4 receptor. Cancer Res. 2010; 70:709–718. [PubMed: 20068161]

Haughian JM, Pinto MP, Harrell JC, Bliesner BS, Joensuu KM, Dye WW, Sartorius CA, Tan AC, Heikkila P, Perou CM, Horwitz KB. Maintenance of hormone responsiveness in luminal breast cancers by suppression of Notch. Proc. Natl. Acad. Sci. USA. 2012; 109:2742–2742. [PubMed: 21969591]

Hennessy BT, Gonzalez-Angulo AM, Stemke-Hale K, Gilcrease MZ, Krishnamurthy S, Lee JS, Fridlyand J, Sahin A, Agarwal R, Joy C, et al. Characterization of a naturally occurring breast cancer subset enriched in epithelial-to-mesenchymal transition and stem cell characteristics. Cancer Res. 2009; 69:4116–4124. [PubMed: 19435916]

Herschkowitz JI, Simin K, Weigman VJ, Mikaelian I, Usary J, Hu Z, Rasmussen KE, Jones LP, Assefnia S, Chandrasekharan S, et al. Identification of conserved gene expression features between murine mammary carcinoma models and human breast tumors. Genome Biol. 2007; 8:R76. [PubMed: 17493263]

Herschkowitz JI, He X, Fan C, Perou CM. The functional loss of the retinoblastoma tumour suppressor is a common event in basal-like and luminal B breast carcinomas. Breast Cancer Res. 2008; 10:R75. [PubMed: 18782450]

Hochgräfe F, Zhang L, O'Toole SA, Browne BC, Pinese M, Porta Cubas A, Lehrbach GM, Croucher DR, Rickwood D, Boulghourjian A, et al. Tyrosine phosphorylation profiling reveals the signaling network characteristics of Basal breast cancer cells. Cancer Res. 2010; 70:9391–9401. [PubMed: 20861192]

Holstege H, Horlings HM, Velds A, Langerød A, Børresen-Dale AL, van de Vijver MJ, Nederlof PM, Jonkers J. BRCA1-mutated and basal-like breast cancers have similar aCGH profiles and a high incidence of protein truncating TP53 mutations. BMC Cancer. 2010; 10:654. [PubMed: 21118481]

Hrabě de Angelis M, McIntyre J 2nd, Gossler A. Maintenance of somite borders in mice requires the Delta homologue DII1. Nature. 1997; 386:717–721. [PubMed: 9109488]

Hvid H, Fels JJ, Kirk RK, Thorup I, Jensen HE, Hansen BF, Oleksiewicz MB. In situ phosphorylation of Akt and ERK1/2 in rat mammary gland, colon, and liver following treatment with human insulin and IGF-1. Toxicol. Pathol. 2011; 39:623–640. [PubMed: 21558470]

Irvine KD. Fringe, Notch, and making developmental boundaries. Curr. Opin. Genet. Dev. 1999; 9:434–441. [PubMed: 10449349]

Jiang Z, Deng T, Jones R, Li H, Herschkowitz JI, Liu JC, Weigman VJ, Tsao MS, Lane TF, Perou CM, Zacksenhaus E. Rb deletion in mouse mammary progenitors induces luminal-B or basal-like/EMT tumor subtypes depending on p53 status. J. Clin. Invest. 2010; 120:3296–3309. [PubMed: 20679727]

Jiang Z, Jones R, Liu JC, Deng T, Robinson T, Chung PED, Wang S, Herschkowitz JI, Egan SE, Perou CM, Zacksenhaus E. RB1 and p53 at the crossroad of EMT and triple-negative breast cancer. Cell Cycle. 2011; 10:1563–1570. [PubMed: 21502814]

Johnston SH, Rauskolb C, Wilson R, Prabhakaran B, Irvine KD, Vogt TF. A family of mammalian Fringe genes implicated in boundary determination and the Notch pathway. Development. 1997; 124:2245–2254. [PubMed: 9187150]

Jones RA, Campbell CI, Gunther EJ, Chodosh LA, Petrik JJ, Khokha R, Moorehead RA. Transgenic overexpression of IGF-IR disrupts mammary ductal morphogenesis and induces tumor formation. Oncogene. 2007; 26:1636–1644. [PubMed: 16953219]

Klinakis A, Szabolcs M, Politi K, Kiaris H, Artavanis-Tsakonas S, Efstratiadis A. Myc is a Notch1 transcriptional target and a requisite for Notch1-induced mammary tumorigenesis in mice. Proc. Natl. Acad. Sci. USA. 2006; 103:9262–9267. [PubMed: 16751266]

Kobayashi S. Basal-like subtype of breast cancer: a review of its unique characteristics and their clinical significance. Breast Cancer. 2008; 15:153–158. [PubMed: 18311481]

Lee CW, Raskett CM, Prudovsky I, Altieri DC. Molecular dependence of estrogen receptor-negative breast cancer on a notch-survivin signaling axis. Cancer Res. 2008a; 68:5273–5281. [PubMed: 18593928]

Lee CW, Simin K, Liu Q, Plescia J, Guha M, Khan A, Hsieh CC, Altieri DC. A functional Notch-survivin gene signature in basal breast cancer. Breast Cancer Res. 2008b; 10:R97. [PubMed: 19025652]

Lee KH, Choi EY, Kim MK, Hyun MS, Jang BI, Kim TN, Kim SW, Song SK, Kim JH, Kim JR. Regulation of hepatocyte growth factor-mediated urokinase plasminogen activator secretion by MEK/ERK activation in human stomach cancer cell lines. Exp. Mol. Med. 2006; 38:27–35. [PubMed: 16520550]

Leong KG, Niessen K, Kulic I, Raouf A, Eaves C, Pollet I, Karsan A. Jagged1-mediated Notch activation induces epithelial-to-mesenchymal transition through Slug-induced repression of E-cadherin. J. Exp. Med. 2007; 204:2935–2948. [PubMed: 17984306]

Lim E, Vaillant F, Wu D, Forrest NC, Pal B, Hart AH, Asselin-Labat ML, Gyorki DE, Ward T, Partanen A, et al. kConFab. Aberrant luminal progenitors as the candidate target population for basal tumor development in BRCA1 mutation carriers. Nat. Med. 2009; 15:907–913. [PubMed: 19648928]

Liu JC, Deng T, Lehal RS, Kim J, Zacksenhaus E. Identification of tumorsphere- and tumor-initiating cells in HER2/Neu-induced mammary tumors. Cancer Res. 2007; 67:8671–8681. [PubMed: 17875707]

Lu X, Kambe F, Cao X, Yamauchi M, Seo H. Insulin-like growth factor-I activation of Akt survival cascade in neuronal cells requires the presence of its cognate receptor in caveolae. Exp. Cell Res. 2008; 314:342–351. [PubMed: 18022157]

Molyneux G, Geyer FC, Magnay FA, McCarthy A, Kendrick H, Natrajan R, Mackay A, Grigoriadis A, Tutt A, Ashworth A, et al. BRCA1 basal-like breast cancers originate from luminal epithelial progenitors and not from basal stem cells. Cell Stem Cell. 2010; 7:403–417. [PubMed: 20804975]

Monaghan-Benson E, Mastick CC, McKeown-Longo PJ. A dual role for caveolin-1 in the regulation of fibronectin matrix assembly by uPAR. J. Cell Sci. 2008; 121:3693–3703. [PubMed: 18957516]

Naldini L, Vigna E, Bardelli A, Follenzi A, Galimi F, Comoglio PM. Biological activation of pro-HGF (hepatocyte growth factor) by urokinase is controlled by a stoichiometric reaction. J. Biol. Chem. 1995; 270:603–611. [PubMed: 7822285]

Niranjan B, Buluwela L, Yant J, Perusinghe N, Atherton A, Phippard D, Dale T, Gusterson B, Kamalati T. HGF/SF: a potent cytokine for mammary growth, morphogenesis and development. Development. 1995; 121:2897–2908. [PubMed: 7555716]

Osipo C, Patel P, Rizzo P, Clementz AG, Hao L, Golde TE, Miele L. ErbB-2 inhibition activates Notch-1 and sensitizes breast cancer cells to a gamma-secretase inhibitor. Oncogene. 2008; 27:5019–5032. [PubMed: 18469855]

Panin VM, Papayannopoulos V, Wilson R, Irvine KD. Fringe modulates Notch-ligand interactions. Nature. 1997; 387:908–912. [PubMed: 9202123]

Parr C, Watkins G, Jiang WG. The possible correlation of Notch-1 and Notch-2 with clinical outcome and tumour clinicopathological parameters in human breast cancer. Int. J. Mol. Med. 2004; 14:779–786. [PubMed: 15492845]

Pece S, Serresi M, Santolini E, Capra M, Hulleman E, Galimberti V, Zurrida S, Maisonneuve P, Viale G, Di Fiore PP. Loss of negative regulation by Numb over Notch is relevant to human breast carcinogenesis. J. Cell Biol. 2004; 167:215–221. [PubMed: 15492044]

Perou CM, Børresen-Dale AL. Systems Biology and Genomics of Breast Cancer. Cold Spring Harb. Perspect. Biol. 2011:3.

Ponzo MG, Lesurf R, Petkiewicz S, O'Malley FP, Pinnaduwage D, Andrulis IL, Bull SB, Chughtai N, Zuo D, Souleimanova M, et al. Met induces mammary tumors with diverse histologies and is associated with poor outcome and human basal breast cancer. Proc. Natl. Acad. Sci. USA. 2009; 106:12903–12908. [PubMed: 19617568]

Ponzo MG, Park M. The Met receptor tyrosine kinase and basal breast cancer. Cell Cycle. 2010; 9:1043–1050. [PubMed: 20237428]

Prat A, Parker JS, Karginova O, Fan C, Livasy C, Herschkowitz JI, He X, Perou CM. Phenotypic and molecular characterization of the claudin-low intrinsic subtype of breast cancer. Breast Cancer Res. 2010; 12:R68. [PubMed: 20813035]

Raafat A, Goldhar AS, Klauzinska M, Xu K, Amirjazil I, McCurdy D, Lashin K, Salomon D, Vonderhaar BK, Egan S, Callahan R. Expression of Notch receptors, ligands, and target genes during development of the mouse mammary gland. J. Cell. Physiol. 2011; 226:1940–1952. [PubMed: 21506125]

Rakha EA, Reis-Filho JS, Ellis IO. Basal-like breast cancer: a critical review. J. Clin. Oncol. 2008; 26:2568–2581. [PubMed: 18487574]

Raouf A, Zhao Y, To K, Stingl J, Delaney A, Barbara M, Iscove N, Jones S, McKinney S, Emerman J, et al. Transcriptome analysis of the normal human mammary cell commitment and differentiation process. Cell Stem Cell. 2008; 3:109–118. [PubMed: 18593563]

Ravid D, Maor S, Werner H, Liscovitch M. Caveolin-1 inhibits cell detachment-induced p53 activation and anoikis by upregulation of insulin like growth factor-I receptors and signaling. Oncogene. 2005; 24:1338–1347. [PubMed: 15592498]

Reedijk M, Odorcic S, Chang L, Zhang H, Miller N, McCready DR, Lockwood G, Egan SE. High-level coexpression of JAG1 and NOTCH1 is observed in human breast cancer and is associated with poor overall survival. Cancer Res. 2005; 65:8530–8537. [PubMed: 16166334]

Reedijk M, Pinnaduwage D, Dickson BC, Mulligan AM, Zhang H, Bull SB, O'Malley FP, Egan SE, Andrulis IL. JAG1 expression is associated with a basal phenotype and recurrence in lymph node-negative breast cancer. Breast Cancer Res. Treat. 2008; 111:439–448. [PubMed: 17990101]

Robinson DR, Kalyana-Sundaram S, Wu YM, Shankar S, Cao X, Ateeq B, Asangani IA, Iyer M, Maher CA, Grasso CS, et al. Functionally recurrent rearrangements of the MAST kinase and Notch gene families in breast cancer. Nat. Med. 2011; 17:1646–1651. [PubMed: 22101766]

Rui L, Emre NC, Kruhlak MJ, Chung HJ, Steidl C, Slack G, Wright GW, Lenz G, Ngo VN, Shaffer AL, et al. Cooperative epigenetic modulation by cancer amplicon genes. Cancer Cell. 2010; 18:590–605. [PubMed: 21156283]

Saal LH, Gruvberger-Saal SK, Persson C, Lövgren K, Jumppanen M, Staaf J, Jönsson G, Pires MM, Maurer M, Holm K, et al. Recurrent gross mutations of the PTEN tumor suppressor gene in breast cancers with deficient DSB repair. Nat. Genet. 2008; 40:102–107. [PubMed: 18066063]

Salani B, Briatore L, Garibaldi S, Cordera R, Maggi D. Caveolin-1 down-regulation inhibits insulin-like growth factor-I receptor signal transduction in H9C2 rat cardiomyoblasts. Endocrinology. 2008; 149:461–465. [PubMed: 18039791]

Sansone P, Storci G, Tavolari S, Guarnieri T, Giovannini C, Taffurelli M, Ceccarelli C, Santini D, Paterini P, Marcu KB, et al. IL-6 triggers malignant features in mammospheres from human ductal breast carcinoma and normal mammary gland. J. Clin. Invest. 2007; 117:3988–4002. [PubMed: 18060036]

Savage K, Lambros MB, Robertson D, Jones RL, Jones C, Mackay A, James M, Hornick JL, Pereira EM, Milanezi F, et al. Caveolin 1 is overexpressed and amplified in a subset of basal-like and metaplastic breast carcinomas: a morphologic, ultrastructural, immunohistochemical, and in situ hybridization analysis. Clin. Cancer Res. 2007; 13:90–101. [PubMed: 17200343]

Shackleton M, Vaillant F, Simpson KJ, Stingl J, Smyth GK, Asselin-Labat ML, Wu L, Lindeman GJ, Visvader JE. Generation of a functional mammary gland from a single stem cell. Nature. 2006; 439:84–88. [PubMed: 16397499]

Shimizu M, Cohen B, Goldvasser P, Berman H, Virtanen C, Reedijk M. Plasminogen activator uPA is a direct transcriptional target of the JAG1-Notch receptor signaling pathway in breast cancer. Cancer Res. 2011; 71:277–286. [PubMed: 21199807]

Smolen GA, Muir B, Mohapatra G, Barmettler A, Kim WJ, Rivera MN, Haserlat SM, Okimoto RA, Kwak E, Dahiya S, et al. Frequent met oncogene amplification in a Brca1/Trp53 mouse model of mammary tumorigenesis. Cancer Res. 2006; 66:3452–3455. [PubMed: 16585167]

Stein D, Wu J, Fuqua SA, Roonprapunt C, Yajnik V, D'Eustachio P, Moskow JJ, Buchberg AM, Osborne CK, Margolis B. The SH2 domain protein GRB-7 is co-amplified, overexpressed and in a tight complex with HER2 in breast cancer. EMBO J. 1994; 13:1331–1340. [PubMed: 7907978]

Stella MC, Trusolino L, Pennacchietti S, Comoglio PM. Negative feedback regulation of Met-dependent invasive growth by Notch. Mol. Cell. Biol. 2005; 25:3982–3996. [PubMed: 15870272]

Stingl J, Eirew P, Ricketson I, Shackleton M, Vaillant F, Choi D, Li HI, Eaves CJ. Purification and unique properties of mammary epithelial stem cells. Nature. 2006; 439:993–997. [PubMed: 16395311]

Stylianou S, Clarke RB, Brennan K. Aberrant activation of notch signaling in human breast cancer. Cancer Res. 2006; 66:1517–1525. [PubMed: 16452208]

Sun T, Aceto N, Meerbrey KL, Kessler JD, Zhou C, Migliaccio I, Nguyen DX, Pavlova NN, Botero M, Huang J, et al. Activation of multiple proto-oncogenic tyrosine kinases in breast cancer via loss of the PTPN12 phosphatase. Cell. 2011; 144:703–718. [PubMed: 21376233]

Taube JH, Herschkowitz JI, Komurov K, Zhou AY, Gupta S, Yang J, Hartwell K, Onder TT, Gupta PB, Evans KW, et al. Core epithelial-to-mesenchymal transition interactome gene-expression signature is associated with claudin-low and metaplastic breast cancer subtypes. Proc. Natl. Acad. Sci. USA. 2010; 107:15449–15454. [PubMed: 20713713]

Visvader JE. Keeping abreast of the mammary epithelial hierarchy and breast tumorigenesis. Genes Dev. 2009; 23:2563–2577. [PubMed: 19933147]

Visvader JE, Smith GH. Murine Mammary Epithelial Stem Cells: Discovery, Function, and Current Status. Cold Spring Harb. Perspect. Biol. 2011:3.

Wagner KU, Wall RJ, St-Onge L, Gruss P, Wynshaw-Boris A, Garrett L, Li M, Furth PA, Hennighausen L. Cre-mediated gene deletion in the mammary gland. Nucleic Acids Res. 1997; 25:4323–4330. [PubMed: 9336464]

Xu K, Nieuwenhuis E, Cohen BL, Wang W, Canty AJ, Danska JS, Coultas L, Rossant J, Wu MY, Piscione TD, et al. Lunatic Fringe-mediated Notch signaling is required for lung alveogenesis. Am. J. Physiol. Lung Cell. Mol. Physiol. 2010; 298:L45–L56. [PubMed: 19897741]

Yalcin-Ozuysal O, Fiche M, Guitierrez M, Wagner KU, Raffoul W, Brisken C. Antagonistic roles of Notch and p63 in controlling mammary epithelial cell fates. Cell Death Differ. 2010; 17:1600–1612. [PubMed: 20379195]

Yamaguchi N, Oyama T, Ito E, Satoh H, Azuma S, Hayashi M, Shimizu K, Honma R, Yanagisawa Y, Nishikawa A, et al. NOTCH3 signaling pathway plays crucial roles in the proliferation of ErbB2-negative human breast cancer cells. Cancer Res. 2008; 68:1881–1888. [PubMed: 18339869]

Zhang N, Gridley T. Defects in somite formation in lunatic fringe-deficient mice. Nature. 1998; 394:374–377. [PubMed: 9690472]

Significance

Here we report that *LFNG*, which suppresses Jagged/Notch signaling in vivo, is consistently expressed at a low level in basal-like tumors and deletion of this gene in the mouse mammary gland enhances accumulation of activated Notch intracellular domain polypeptides, increases proliferation, and induces basal-like mammary tumors in cooperation with amplification of the *Met/Caveolin* gene locus. These mutations interact to promote a specific BLBC signaling network with increased Notch pathway activation, as well as elevated Met and Igf-1R signaling. Patients with *MET/CAV*-overexpressing BLBC may therefore benefit from combination therapy targeting Notch, MET, and IGF1R.

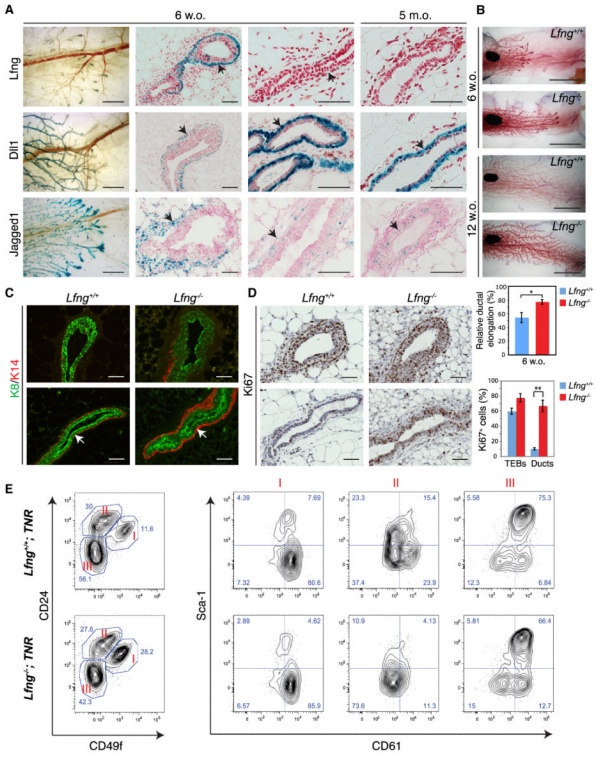

Figure 1. *Lfng* Is Expressed in Mammary Basal Cells and Its Deletion Causes Increased Proliferation and Expansion of the CD24^{+}CD49f^{Hi}CD61^{+}Sca1^{-} Population in the Pubescent Mammary Gland

(A) Expression of *Lfng*, *Dll1*, and *Jagged1* in the mouse mammary gland. Shown are representative photomicrographs of whole-mount (left column) and sectioned X-Gal staining of mammary glands from *Lfng*$^{LacZ/+}$, *Dll1*$^{LacZ/+}$, and *Jagged1*$^{\beta-Geo/+}$ virgin mice at 6 weeks and 5 months of age. Sections for the TEBs are shown in the second column from left.

(B) Mammary hyperplasia in the *Lfng*$^{-/-}$ mutant. Shown are representative photomicrographs of whole-mount mammary glands from 6- and 12-week-old virgins.

(C) Representative photomicrographs of anti-K8, −K14 immunofluorescence staining in mammary sections from 6-week-old virgins of *Lfng*$^{+/+}$ and *Lfng*$^{-/-}$ mice. TEBs and ducts are shown in upper and lower panels, respectively.

(D) Ductal elongation at 6 weeks old, measured as the distance between the lymph node and the ductal front line normalized to the distance between the lymph node and the end of the fat pad, are presented as mean values ± standard error. *$p < 0.05$. Note, the *Lfng* null allele was generated through expression of Cre in the germline of female *Lfng*$^{flox/+}$; MMTV-Cre mice. Increased mammary epithelial proliferation in *Lfng*$^{-/-}$ compared with control *Lfng*$^{+/+}$ littermates. Shown are representative photomicrographs of anti-Ki67 immunostaining in mammary sections same as (C). Numbers of Ki67^{+} cells are normalized to the total number of epithelial cells in TEBs or in ductal areas, presented as mean values ± standard error. **$p < 0.005$.

(E) Representative flow cytometry analyses of lineage-depleted mammary cells from *Lfng*$^{-/-}$*; TNR* mutants compared with *Lfng*$^{+/+}$*; TNR* littermates at 6 weeks old. Shown are CD24/CD49f plots and Sca-1/CD61 plots on populations I, II, III gated as in CD24/CD49f plots.

Scale bars correspond to 1 mm in left panels of (A), 5 mm in (B), and 50 μm in all others. See also Figure S1.

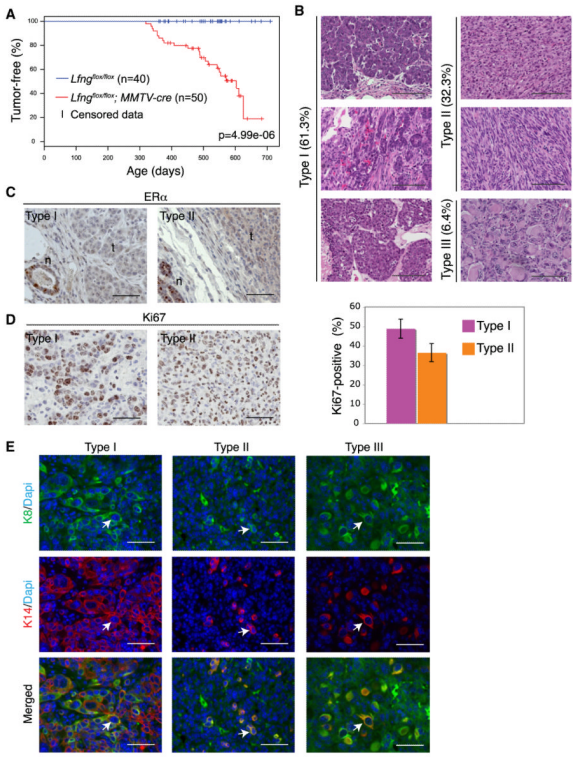

Figure 2. Deletion of *Lfng* Induced Mammary Tumors in Mice

(A) Kaplan-Meier mammary tumor-free survival curve for control *Lfng*$^{flox/flox}$ and *Lfng*$^{flox/flox}$*; MMTV-Cre* conditional mutant mice.

(B) Representative photomicrographs of H&E stained sections showing three histological types of *Lfng*$^{flox/flox}$*; MMTV-Cre* mammary tumors.

(C) Anti-ERα immunostaining on two main types of *Lfng*$^{flox/flox}$*; MMTV-Cre* mammary tumors. n: normal tissue; t: tumor. Note positive ERα staining in normal tissue adjacent to the tumor.

(D) Representative photomicrographs and quantification of anti-Ki67 immunostaining on two main types of *Lfng*$^{flox/flox}$*; MMTV-Cre* mammary tumors. Data are derived from two sections in each of three Type I and Type II tumors presented as mean values ± standard error.

(E) Representative photomicrographs of anti-K8, −K14 immunofluorescence staining on three types of *Lfng*$^{flox/flox}$*; MMTV-Cre* mammary tumors. Arrows point to cells showing co-expression of K8 and K14.

Scale bars correspond to 100 μm in (B), 50 μm in (C), (D) and (E).

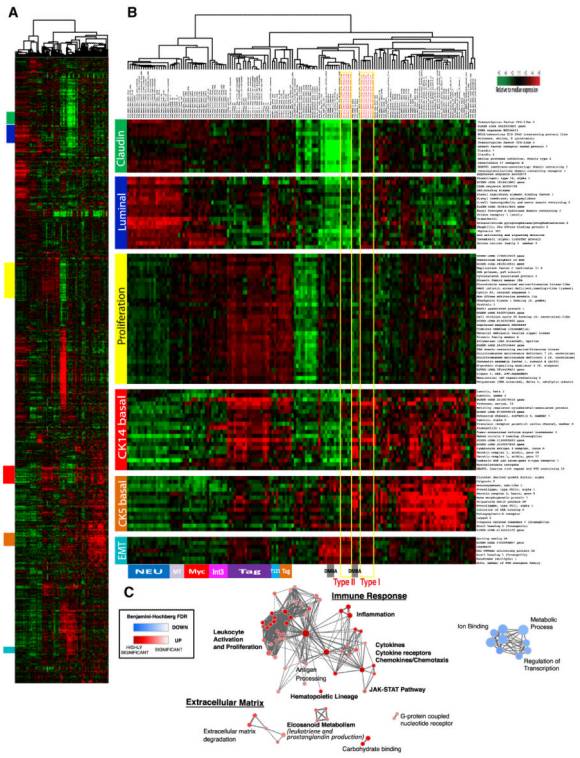

Figure 3. *Lfng*$^{flox/flox}$; *MMTV-Cre* Tumors Cluster with Basal-like and Claudin-Low Mouse Mammary Tumor Models

(A) Overview of expression of reference genes in tumors from various mouse models of breast cancer, including 11 tumors from *Lfng*$^{flox/flox}$; *MMTV-Cre* mice. Colored bars at left correspond to regions shown in (B).

(B) Expression of selected genes representing the Claudin gene cluster, luminal gene cluster, proliferation-associated gene cluster, CK14 basal-like gene cluster, CK5 basal-like gene cluster, and EMT gene cluster. Expression data from type I and type II *Lfng*$^{flox/flox}$; *MMTV-Cre* tumors are contained within yellow boxes. Clusters of tumor models are highlighted at the bottom. DMBA, 7,12-dimethylbenz[a]-anthracene.

(C) Enrichment map for gene sets over-represented in list of genes that are differentially expressed comparing *Lfng*$^{flox/flox}$; *MMTV-Cre* mouse mammary tumors to other mouse models of breast cancer.

See also Table S1.

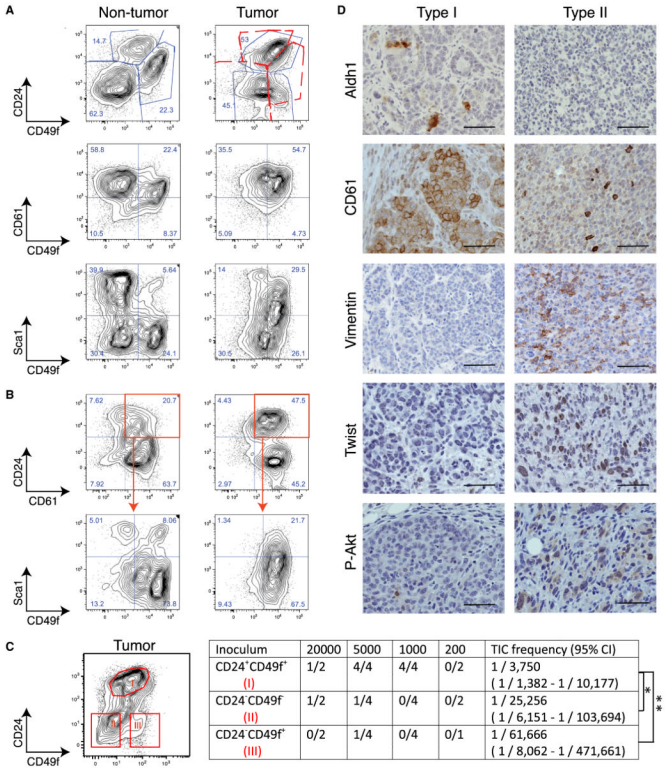

Inoculum	20000	5000	1000	200	TIC frequency (95% CI)
$CD24^+CD49f^+$ (I)	1/2	4/4	4/4	0/2	1 / 3,750 (1 / 1,382 - 1 / 10,177)
$CD24^+CD49f^-$ (II)	1/2	1/4	0/4	0/2	1 / 25,256 (1 / 6,151 - 1 / 103,694)
$CD24^-CD49f^+$ (III)	0/2	1/4	0/4	0/1	1 / 61,666 (1 / 8,062 - 1 / 471,661)

Figure 4. Flow Cytometry and Immunohistological Analysis of *Lfng$^{flox/flox}$; MMTV-Cre* Tumors

(A) Representative flow cytometry contour plots for lineage-depleted mammary tumor cells compared with non-tumor lineage-depleted mammary cells from a *Lfng$^{flox/flox}$; MMTV-Cre* mouse. Shown are CD24/CD49f, CD61/CD49f, and Sca1/CD49f plots from a Type I tumor.

(B) Additional analysis of the flow cytometry data as shown in (A): CD24/CD61plots and Sca1/CD49f plots on the $CD24^+CD61^+$ populations as gated in the upper panels.

(C) Limiting dilution transplantation assay on $CD24^+CD49f^+$, $CD24^-CD49f^-$ and $CD24^-CD49f^+$ tumor cells as gated in a CD24/CD49f plot. Data are derived from two independent experiments using two donors of type I tumor. TIC: Tumor-Initiating Cells. *p = 0.0307 ($CD24^+CD49f^+$ versus $CD24^-CD49f^-$), **p = 0.0155 ($CD24^+CD49f^+$ versus $CD24^-CD49f^+$)

(D) Representative photomicrographs of anti-Aldh1, anti-CD61, anti-Vimentin, anti-Twist and anti-Phospho-Akt immunostaining in two main types of *Lfng$^{flox/flox}$; MMTV-Cre* mammary tumors. Scale bars correspond to 50 μm.

See also Figure S2.

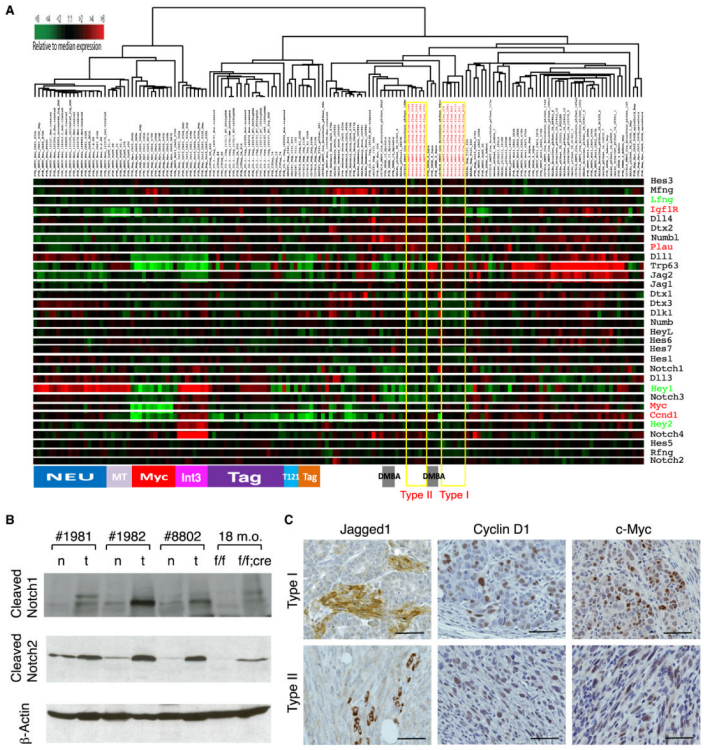

Figure 5. Dysregulation of Notch Signaling Pathway and Downstream Target Genes in *Lfng*$^{flox/flox}$; *MMTV-Cre* Tumors

(A) Expression of selected Notch signaling pathway and downstream target genes in tumors from various mouse models of breast cancer, including 11 tumors from *Lfng*$^{flox/flox}$; *MMTV-Cre* mice. Expression data from type I and type II *Lfng*$^{flox/flox}$; *MMTV-Cre* tumors are contained within yellow boxes. Genes with lower expression in *Lfng*$^{flox/flox}$; *MMTV-Cre* tumors are highlighted in green, with higher expression in red. Clusters of tumor models are highlighted at the bottom. DMBA, 7,12-dimethylbenz[a]-anthracene.

(B) Western blot analysis of cleaved Notch1 and cleaved Noch2 in mammary tumors (t) and non-tumor mammary tissue (n) from *Lfng*$^{flox/flox}$; *MMTV-Cre* mice (#1981, #1982, #8802), as well as in non-tumor mammary tissues from 18-month old *Lfng*$^{flox/flox}$ and *Lfng*$^{flox/flox}$; *MMTV-Cre* littermate mice. β-actin served as loading control.

(C) Representative photomicrographs of anti-Jagged1, anti-Cyclin D1 and anti-C-Myc, immunostaining in two main types of *Lfng*$^{flox/flox}$; *MMTV-Cre* mammary tumors. Scale bars correspond to 50 μm.

See also Figure S3.

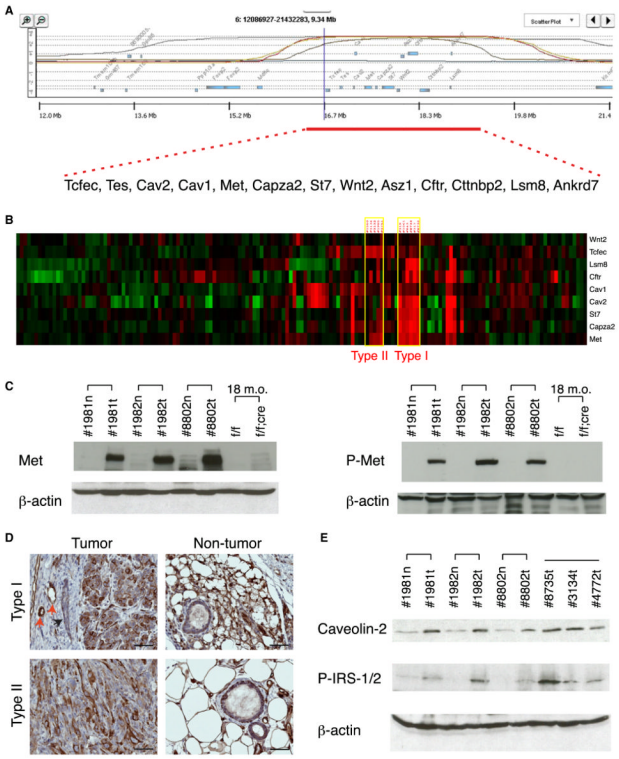

Figure 6. Met/Caveolin Amplicon and Signaling of Met and IgfR in *Lfng*$^{flox/flox}$; *MMTV-Cre* Mammary Tumors

(A) aCGH analysis of DNA isolated from four *Lfng*$^{flox/flox}$; *MMTV-Cre* mouse tumors and one *Lfng*$^{flox/+}$; *MMTV-Cre* tumor showing a commonly amplified locus among all four *Lfng*$^{flox/flox}$; *MMTV-Cre* tumors on chromosome 6. Red bar corresponds to the overlapping region containing 13 genes.

(B) Expression of the commonly amplified genes as shown in (A) in 11 *Lfng*$^{flox/flox}$; *MMTV-Cre* tumors in comparison with expression of these genes in other mouse models of breast cancer. Expression data from type I and type II *Lfng*$^{flox/flox}$; *MMTV-Cre* tumors are contained within yellow boxes.

(C) Western blot analysis of Met and phospho-Met in mammary tumors (t) and non-tumor mammary tissue (n) from *Lfng*$^{flox/flox}$; *MMTV-Cre* mice (#1981, #1982, #8802), as well as in mammary tissue from 18-month old *Lfng*$^{flox/flox}$ and *Lfng*$^{flox/flox}$; *MMTV-Cre* littermate mice. β-actin served as loading control.

(D) Representative photomicrographs of anti-Caveolin-1 immunostaining in two main types of *Lfng*$^{flox/flox}$; *MMTV-Cre* mammary tumors. Red arrows indicate positive staining in blood vessels. Black arrow points to a mammary duct adjacent to the tumor. Note, non-tumor mammary tissues show strong staining in adipocytes and weak staining in myoepithelial cells. Scale bars correspond to 50 μm.

(E) Western blot analysis of Caveolin-2 and Phospho-IRS-1/2 in mammary tumors (t) and non-tumor mammary tissue (n) from *Lfng*$^{flox/flox}$; *MMTV-Cre* mice.

See also Figure S4.

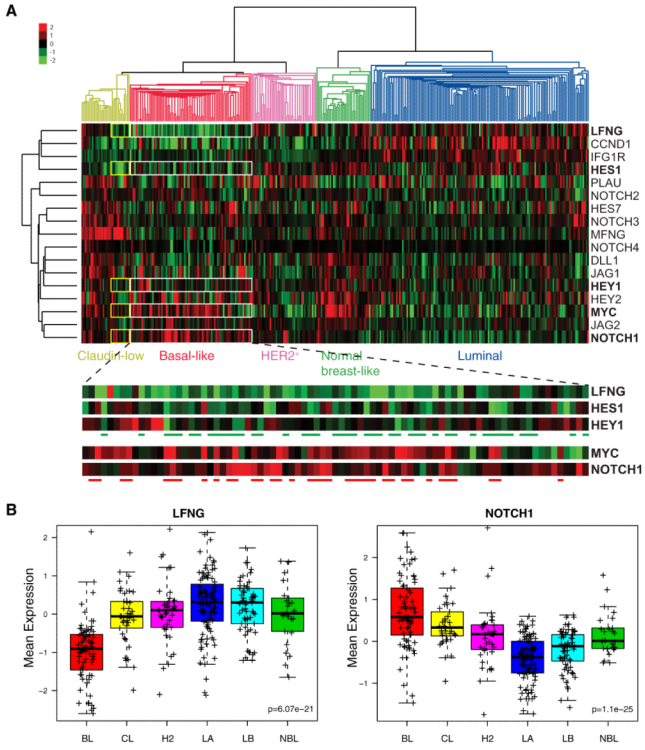

Figure 7. Human Basal-like and A Subset of Claudin-Low Breast Cancers Exhibit Low Levels of *LFNG, HES1*, and *HEY1* Gene Expression, but High Levels of *NOTCH1* and *MYC* Gene Expression

(A) Expression of selected Notch pathway genes and proliferation-associated Notch target genes in 320 breast tumors and 17 normal breast samples from the North Carolina data set. 5 subtypes of human breast cancers are highlighted. Expression of *LFNG, HES1*, *HEY1, MYC* and *NOTCH1* in basal-like breast cancers are boxed in white and shown in enlarged view (bottom of panel A). Expression levels for these five genes in a subset of Claudin-low breast cancers (with lower LFNG levels) are boxed in yellow. Green bars mark individual tumors showing decreased expression of all three genes (*LFNG, HES1*, *HEY1*). Red bars mark tumors with increased expression of both *NOTCH1* and *MYC*.

(B) Mean expression values for *LFNG* and *NOTCH1* from the North Carolina data set. BL, basal-like; CL, Claudin-low; H2, HER2-positive; LA, luminal A; LB, luminal B; NBL, normal breast-like. p values were calculated by comparing expression means across all subtypes.

See also Figure S5.

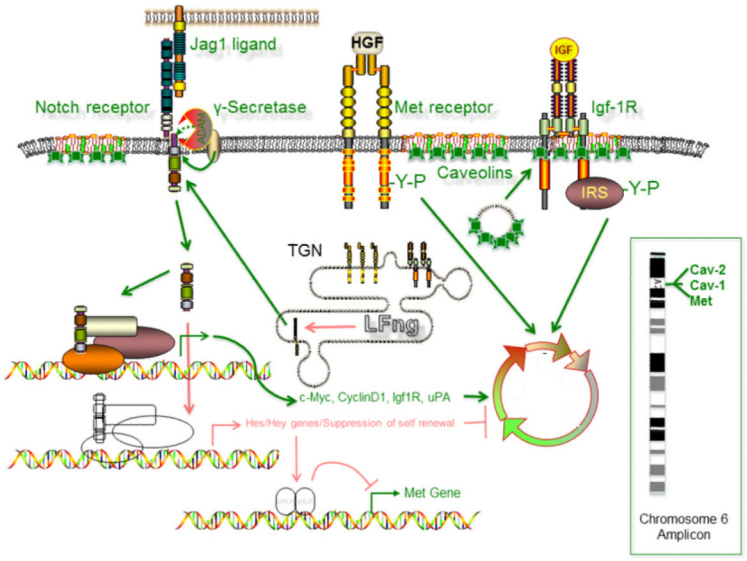

Figure 8. Model of Cooperation between Lfng Deficiency and Met/Caveolin Amplification/ Overexpression in Basal-like Breast Cancer

Lfng modifies Notch receptor to inhibit its activation by Jagged ligand and enhance its activation by Dll ligand. Loss of *Lfng* results in increased Jagged1-mediated Notch activation and upregulation of c-Myc, Cyclin D1, Igf1R and uPA, leading to increased proliferation. Loss of *Lfng* may decrease Dll1-mediated Notch activation in bipotent mammary progenitor cells, causing expansion of basal cells. Decreased expression of Hes/Hey Notch target genes may de-repress the Met promoter. Selected as cooperative event in *Lfng* deficiency induced mammary tumorigenesis, the Met/caveolin amplicon increases abundance of Met and Caveolin1/2, the latter proteins are predicted to enhance signaling through Igf-1R and IRS. Signaling through Met and Igf-1R stimulate proliferation. TGN, trans Golgi network.